Observations of Turbulent Flow Fields in the Chesapeake Bay Estuary for Tidal Energy Conversion

Luksa Luznik
Karen A. Flack
Department of Mechanical Engineering
U.S. Naval Academy
Annapolis, MD USA

***Abstract*-This paper presents preliminary results from a two-week long set of field experiments performed to characterize flow structure and turbulence in the mid-water column during tidal flows in the Chesapeake Bay estuary. At the deployment location, in the vicinity of Kent Island peak flood/ebb tidal flows range from +/- 40 cm/s in the along-channel direction and secondary flow in the cross-channel direction reaches peak of +/-10 cm/s during the slack parts of a tidal cycle. Conditionally sampled mean velocity profiles indicate asymmetry in the flood/ebb tidal flows, which is attributed to the tidal straining. Temporal velocity spectra are presented and show modifications of the turbulence spectra due to presence of surface gravity wave field. Time history of turbulent kinetic energy dissipation rate shows variations on a tidal time scale with magnitudes ranging from 10^{-6} to 10^{-3} m^2/s^3. Results are discussed in the context of tidal turbine design and performance.**

I. INTRODUCTION

Hydrokinetic energy devices are gaining increasing attention as a source of renewable energy. Tidal turbines capture the kinetic energy in the water during flood and ebb tidal flows. The energy conversion is similar to that of wind turbines with the significant advantage of water turbines having much higher power densities. While wind turbines are a fairly mature technology with many commercial applications, tidal turbines are still in the research and development phases, with limited full-scale data for performance assessments.

Understanding and proper representation of the flow structure and turbulence in flood/ebb currents are fundamental to our understanding of the working conditions of tidal turbines. Currently there is paucity of turbulence measurements that cover not only bottom boundary layer but also mid-water column where these devices might operate [1]. The upstream turbulent flow fields that coincide with energy containing scales (diameters of rotor blades range from 1 m – 25 m) is an important issue in the design of tidal turbines in the areas of maximum load prediction, structural excitation, fatigue, control schemes and power quality. Large-scale coherent turbulence can cause excessive loads on blades, necessitating higher structural integrity for blades and drive trains, and potentially the inclusion of control schemes such as active pitching or passive stall. Smaller scale turbulence also contributes to the fatigue since the turbine blades experience an unbalanced cyclic load resulting from rotation of the blades through a sheared turbulent velocity profile. Hence, the power quality is greatly improved by placing these devices in areas of high flow rates with low turbulence.

Measurements of ocean turbulence are difficult to obtain because of variety of technical challenges including the contamination of turbulence signal by wave motions, and lack of spatial resolution [2]. Most commonly used devices are Acoustic Doppler Current Profiler (ADCP) [3, 4, 5] and the Acoustic Doppler Velocimeter (ADV) [6]. The former provides vertical distribution of three-dimensional velocity in equally spaced vertical bins typically 0.25 to 0.5m resolution, while the latter is a point measurement technique with higher spatial resolution. Recently, high resolution pulse coherent profilers have become commercially available that combine simultaneous spatial measurements with high spatial resolution, e.g. vertical velocity bins within 2 to 3 cm. The Nortek HR profiler used in this work is discussed further in the next section.

A number of additional measurement techniques have been used to investigate the bottom boundary layer. The Benthic Acoustic Stress Sensor (BASS), a system based on measuring the acoustic travel time has been continually improved in order to measure the velocity from bottom- mounted tripods [7, 8]. Laser Doppler Velocimetry (LDV) has been utilized by [9] in the wave bottom boundary layer, and Particle Image Velocimetry (PIV) has been used successfully in bottom boundary layer studies of the coastal ocean [10, 11]. The data obtained using these sensors constitute the current state of knowledge on the turbulence in the coastal ocean.

This paper discusses preliminary data from a two-week long set of field experiments performed in the vicinity of Kent Island in the Chesapeake Bay estuary to characterize flow structure and turbulence in the water column and the bottom boundary layer during flood/ebb tidal flows. These results will also be used to address the feasibility of this location for deployment of a prototype turbine. The paper is organized as follows: Section II discusses the experimental set up and introduces acquired data. Section III describes data analysis and Section IV presents mean velocity profiles, and turbulence parameters including temporal spectra and dissipation of turbulence kinetic energy.

II. MEASUREMENTS

Instrumentation

The bottom tripod outfitted for the deployment discussed in this paper is shown in Figure 1 and includes the following instrumentation: two vertically oriented Nortek USA ADV's, vertically oriented Nortek high resolution (HR) pulse coherent profiler, two YSI conductivity temperature sondes and two HOBO pressure transducers. Table 1 shows the sampling volume locations and the sampling rate of the major sensors mounted on the tripod. Auxiliary data from ADV's and HR profiler include sensors' pitch, roll, pressure and temperature sampled at 1 Hz. The HR profiler has a vertical resolution of 30 mm, and with 38 velocity bins covers just over 1m of the water column. The Acoustic Wave and Current Meter, (AWAC) mounted on a separate tripod frame is used to provide current profiles and wave directional system. All instruments were synchronized using the acquisition computer clock as a reference, except for the pair of ADV's which were configured to start data collection exactly at the same time via hardware connection. For the purposes of this paper only ADV and HR profiler data will be discussed.

Figure 1.Bottom tripod with onboard instrumentation prior to deployment.

TABLE I
SENSORS, LOCATIONS AND SAMPLING RATE

Equipment	Signal[a]	Sampling Rate	Location[a] (m)
Nortek ADV#1	u,v,w	16 Hz	1.7
Nortek ADV#2	u,v,w	16 Hz	0.8
Nortek HR Profiler	u,v,w	2 Hz	1.6-2.6
YSI CTD #1	T, S	1 sample/5min	0.8
YSI CTD #2	T, S	1 sample/5min	0.4
HOBO #1	P	1 Hz	1.4
HOBO #2	P	1 Hz	1.0
Nortek AWAC	u,v,w, waves	1 profile/5 min	0.6-surface

[a] The nomenclature used are: u,v,w velocities in the instrument frame of reference; T, temperature measured, S salinity measured, P pressure measured. Locations are given in elevation above the seabed.

Acquired Data and Flow Conditions

Measurements described here were collected from 7-20 July 2010 in the vicinity of Kent Island, at location 38° 51.38'N; 76° 23.12'W, about 3 nautical miles SE (south-east) from Annapolis MD in a nominal water depth of 5 m. This site was selected for several reasons:

1) The current speeds at this location are strong, up to 1-2 knots, particularly close to the water surface. This is desirable considering that some types of turbines begin to produce power at ~1 m/s currents.
2) The seabed at this location is hard and consists of sand and shell, which is advantageous for potential future use of this location for deployment of a prototype turbine.
3) The site is in the vicinity of NOAA Thomas Point meteorological station which provides real-time meteorological data. Figure 2 shows the wind speed record for the duration of the experiment.

During the deployment USNA divers assisted the placement and orientation of the tripod on the bottom. Once lowered, the platform heading was oriented 45° with respect to Magnetic North. This orientation ensures that during flood/ebb currents instruments are not in the wake of the platform. The recovery of the system showed that the instruments have become fouled substantially over the course of the deployment. However, as discussed in the next section, analysis so far shows no deterioration of data quality with time.

ADV's and HR profiler measurements were obtained in "bursts" lasting for 20 minutes followed by 30 minutes of instrument downtime. All other supporting sensors sampled continuously. Overall, for two ADVs data include 325 bursts covering over 108 hours of continuous data collection. The HR profiler stopped collecting data in early hours of July 19 due to full hard drive memory resulting in total of 305 velocity bursts.

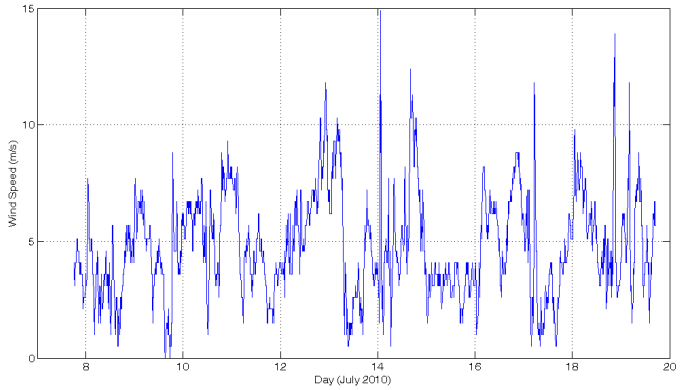

Figure 2. Wind Speed. Time is given in decimal days (GMT time). Data Source: NOAA National Data Buoy Center web site, Station TPLM2-Thomas Point.

III. Data Analysis

In the analysis that follows, instantaneous values of velocity (u, v, w) in the x, y, z directions correspond to the instrument frame of reference. Velocities in each 20-minute burst were rotated into along-channel, and cross-channel components using the principal component analysis [12]. This would be equivalent to aligning the turbine axis in the direction of the strongest flow. In this system x and y are coordinates in the downstream and cross-stream directions and z is the vertical coordinate, positive upward with z=0 at the seabed. These rotated velocities are used throughout this paper. U, V and W denote burst averaged velocities, that is, time averaged velocities over the length of the burst, i.e. 20 minutes, and u', v', w' denote turbulent fluctuations.

The misalignment of the velocity sensors which occurs in the process of setting up the bottom tripod was corrected based on the pitch and roll data, and data post processing include a quality check with a rejection threshold on instantaneous velocities with less than 60% correlation in velocity calculations. This resulted in less than 5% data rejection.

IV. Results

Mean Velocity Profiles

Figure 3a shows the temporal variation of burst-averaged velocity components along-channel (U), cross-channel (V) and vertical axis (W) from a single ADV at z=1.7 m. Figure clearly shows strong semidiurnal tidal currents with mean along-channel velocity ranging between +/-40 cm/s. Currents closer to the surface, outside of the bottom boundary layer will be higher. While this level of current would not support a large scale tidal turbine, the site could be used for testing of smaller scale turbine with lower cut-in speeds. Mean cross-channel velocity (V) reaches a maximum of about +/-10 cm/s and vertical mean velocities are small ~1 to 2 cm/s. Cross-channel velocities (V) are small and occur mostly at times during slack periods of a tidal cycle. Hence, flow at this location in the Chesapeake Bay is mainly along the channel axis but secondary flow is still evident.

Time history of burst averaged water depth derived from ADV pressure record is shown in Figure 3b. At the deployment location average water depth is 5.5 m with tidal variations of about +/-0.5 m, which is typical for the Chesapeake Bay [13]. There is a slight but noticeable phase difference between tidal elevation and tidal velocities. Peak flood (+ve U) occurs before high water, and peak ebb (-ve U) occurs before low water.

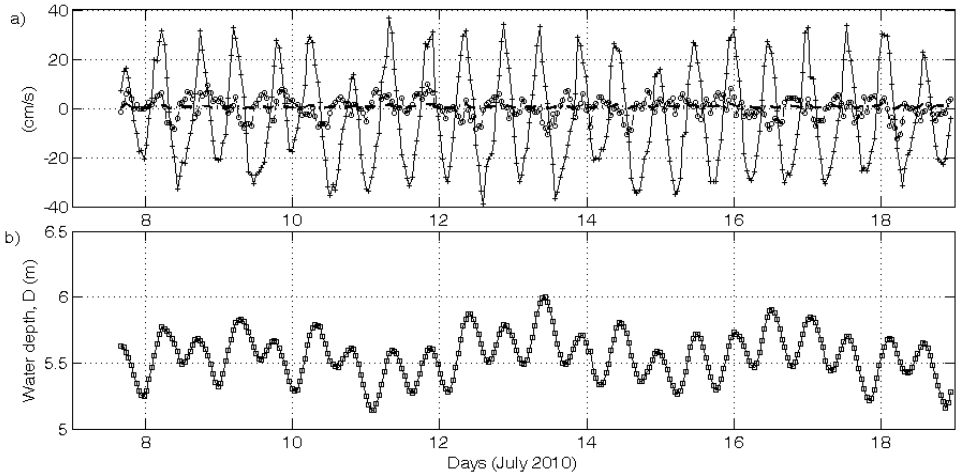

Figure 3. a) Temporal variation of mean along-channel U (+), cross-channel V (o), and vertical W (solid line) velocities from ADV#1 located at z =1.68m above the seabed. b) Temporal variation of burst averaged water depth derived from ADV pressure record. Note that mean vertical velocity is small (~1-2 cm/s).

To examine the ebb/flood tidal flows in more detail, Figure 4 presents the profiles of ensemble averaged along-channel velocity against normalized elevation z/D, with D=5.5m, the overall mean water depth. Ensemble averaging is performed by taking all profiles during the two-week deployment with a burst averaged U between 10 and 20 cm/s and averaging them together to produce a single profile. This is repeated in 10 cm/s increments from –50 to 40 cm/s, resulting in nine ensemble-averaged profiles. Table 2 shows the number of bursts used in the ensemble averaging process.

TABLE II
ENSEMBLE AVERAGING STATISTICS

Velocity Range (cm/s)	# of 20 min bursts in ensemble
-40 to -50	1
-40 to -30	33
-30 to -20	58
-20 to -10	54
-10 to 0	32
0 to10	34
10 to 20	40
20 to 30	35
30 to 40	21

The velocity profiles during ebb and flood flows differ notably. The peak ebb profile exhibits nearly linear variation with height, whereas peak flood profile does not. This observed asymmetry is most likely related to tidal straining [14, 15]. At the lowest elevations ebb profiles show abrupt change in slope (circled area in Figure 4). Explanation for this abrupt change in slope is that during ebb flow, the lowest velocity bins of the HR profiler sensor were in the wake of the tripod frame.

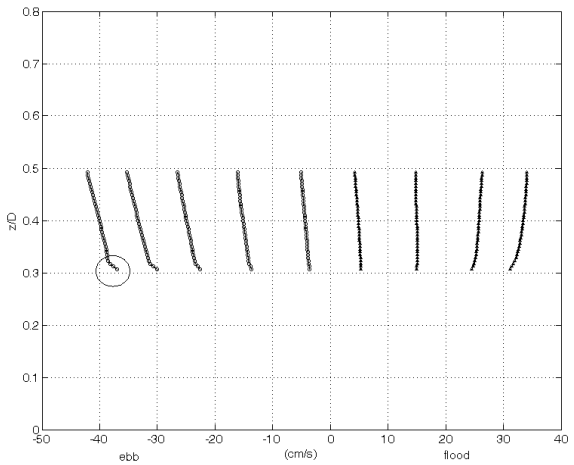

Figure 4. Ensemble averaged mean along shore velocity. Note that slope change in the lowest portion of the ebb profiles is a consequence of HR sensor lowest velocity bins being in the tripod frame wake.

Velocity Spectra

Representative temporal velocity spectra of $\langle u'^2 \rangle$, $\langle v'^2 \rangle$, and $\langle w'^2 \rangle$, where $\langle\ \rangle$ indicate time averaging are presented in Figure 5. Spectra are calculated from a single burst (19200 points) using blocks of 512 points (i.e. 32 seconds of data), 50% overlap and Hamming windowing. Prior to FFT analysis the burst means were removed from the instantaneous velocity data. Presented spectra are representative of peak flood currents with and without surface gravity waves present. Note that corresponding wind velocities shown in Figure 2 for these two times are 9 and 4 m/s. In Figure 5b, turbulent spectra show peaks at about 0.3 Hz, which is representative of a wave signature, in this case wind generated waves with ~3 second period. Waves typically have much larger spatial scales than the turbulence but the frequency of the orbital wave motion falls within the turbulence spectrum, since the wave speed is much higher than the typical flow. Thus, peaks in Figure 5b represent wave induced velocities, and are much larger than the turbulent fluctuations. In Figure 5a, spectra do not show fluctuations corresponding to wave signature and have a clear Kolmogorov –5/3 spectral slope indicative of inertial range of turbulence [16].

Calculations of vertical turbulent stresses, $\langle u'w' \rangle$ and $\langle v'w' \rangle$ are not presented in this paper. It is important to mention that because of presence of wave signature in the velocity data, calculations of turbulent stresses require special attention. References [17 18] present technique based on simultaneous measurements using two spatially separated velocity sensors that eliminates wave effects in the estimates of Reynolds stresses. Present set up allows for this technique to be used and will be reported in the future.

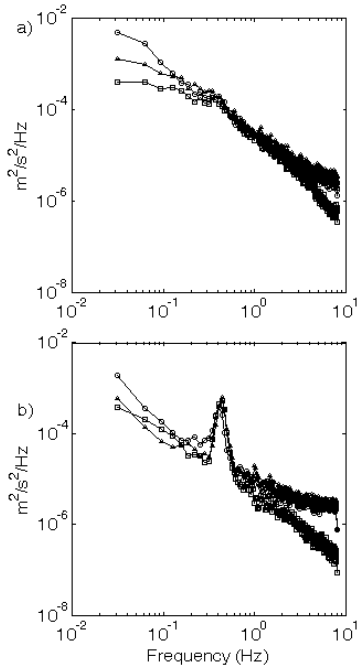

Figure 5. Velocity spectra Suu, Svv and Sww as a function of cyclic frequency. Spectra are obtained from ADV #1 (hab = 1.7 m) velocity data. a) burst #43 corresponding to high mean flow and weak surface gravity wave field; b) burst #106 corresponding to high mean flow and strong surface gravity wave field.

Dissipation estimates

Estimates of turbulent kinetic energy (TKE) dissipation rate, ε is obtained indirectly from inertial subrange spectra of vertical velocity data (S_{ww}) following [19] and [20] and are presented in Figure 6. Magnitudes range from 10^{-6} to 10^{-3} m^2/s^3 and vary with the tidal cycle. Variation in TKE dissipation magnitude on a tidal cycle time scale is most likely related to the variation in turbulence generation over the same period. Shear production of turbulence is related to the mean shear working against the Reynolds stress [21] and we have already shown that mean shear varies considerably over the tidal cycle. In the future we will calculate variation of Reynolds stresses, and possibly be able to confirm tidal variation in turbulence production.

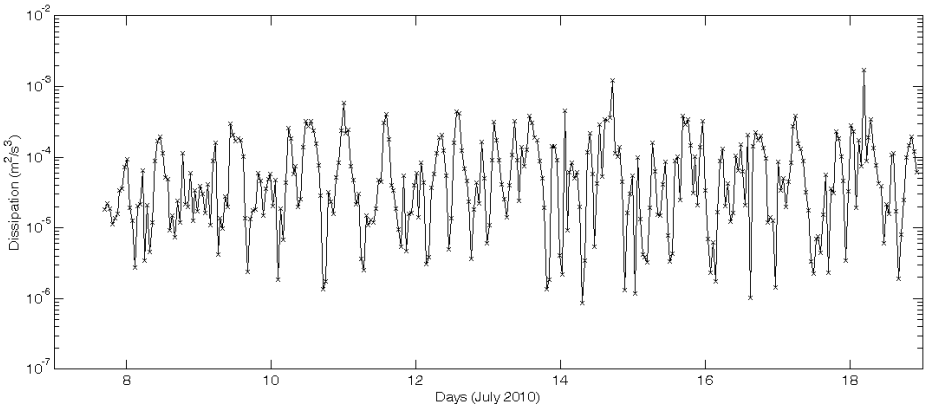

Figure 6. Time history of the turbulent kinetic energy dissipation rate, ε over the duration of the deployment. Variations on the tidal time scale can be observed. Note that vertical axis is log scale.

V. DISCUSSION

In this paper we presented preliminary results from a recent deployment in the Chesapeake Bay with the aim to elucidate complexity of flow conditions during flood/ebb tidal flows. Tidal turbines, if placed in such flows will be exposed not only to tidal time-scale variations in flow magnitudes, but also to spatially and temporally varying turbulence. As demonstrated, mean shear in the mid-water column is substantial during peak flows, thus turbine blade would experience substantial variation in the incoming flow. As reference [22] suggest, this would require continuous blade pitch adjustments for optimal performance. The measurements clearly indicate that waves influence the flow field in a substantial way. The resulting impact on tidal turbine performance is still unknown and requires systematic investigation.

ACKNOWLEDGMENT

This work is supported in full by the Office of Naval Research Grant #: N00014-10-WX21317 and in part by the U.S. Naval Academy Research Council. The authors thank Louise Wallendorf for useful technical advice and help during the deployment/recovery of the tripod. We also thank the captain of the "Metal Shark" and Annapolis Naval Station Dive Locker who provided support for the project.

REFERENCES

[1] L.E. Myers and A.S. Bahaj, "Experimental analysis of the flow field around horizontal axis tidal turbines by use of scale mesh disk rotor simulators," O*cean Engineering,* vol. 37, pp. 218-227, 2010.

[2] W.D. Grant and O.S. Madsen, " The continental shelf bottom boundary layer," *Annu. Rev Fluid Mech*., vol. 18, pp.265-303, 1986..

[3] A. Lohrmann, B. Hackett, and L. P. Roed, "High-resolution measurements of turbulence, velocity and stress using a pulse-to-pulse coherent sonar," *Journal of Atmospheric and Oceanic Technology*, vol 7, pp.19–37, 1990.

[4] Y. Y. Lu and R. G. Lueck, "Using a broadband ADCP in a tidal channel. part I: Mean flow and shear," *Journal of Atmospheric and Oceanic Technology*, vol 16, pp.1556–1567, 1999.

[5] T. P. Rippeth, E. Williams, and J. H. Simpson, "Reynolds stress and turbulent energy production in a tidal channel," *Journal of Physical Oceanography*, vol. 32, pp.1242–1251, 2002.

[6] G. Voulgaris and J. H. Trowbridge, "Evaluation of the acoustic doppler velocimeter (ADV) for turbulence measurements," *Journal of Atmospheric and Oceanic Technology*, vol. 15, pp.272–289, 1998.

[7] A. Williams, J. Tocho, R. Koehler, T. Gross, W. Grand, and D. C.V.R, "Measurements of turbulence with an acoustic current meter array in the oceanic bottom boundary layer," *Journal of Atmospheric and Oceanic Technology*, vol. 4, pp. 312–327, 1987.

[8] T. F. Gross, A. J. Williams, and E. A. Terray, "Bottom boundary-layer spectral dissipation estimates in the presence of wave motions," *Continental Shelf Research*, vol. 14, pp.1239–1256, 1994.

[9] J. H. Trowbridge and Y. C. Agrawal, "Glimpses of a wave boundary-layer,". Journal of Geophysical Research-Oceans, vol. 100, pp. 20729–20743, 1995.

[10] L. Bertuccioli, G. I. Roth, J. Katz, and T. R. Osborn, "A submersible particle image velocimetry system for turbulence measurements in the bottom boundary layer," *Journal of Atmospheric and Oceanic Technology*, vol. 16, pp.1635–1646, 1999.

[11] L. Luznik, R. Gurka, W. A. M. Nimmo Smith, W. Zhu, J. Katz, and T. R. Osborn, "Distribution of energy spectra, Reynolds stresses, turbulence production, and dissipation in a tidally driven bottom boundary layer," *Journal of Physical Oceanography*, vol. 37, pp.1527–1550, 2007.

[12] J. Emery, R. Thompson, "*Data analysis methods in Physical Oceanography*,"Pergamon 634 pp.

[13] W.Q., Lin, L.P., Sanford, S.E., Suttles and R. Valigura, "Drag coefficients with fetch-limited wind waves," *Journal of Physical Oceanography*, vol. 32 pp. 3058–3074, 2002.

[14] Simpson J.H., Brown, J. Matthews, J., and G. Allen, "Tidal straining, density currents, and stirring in the control of estuarine stratification," *Estuaries*, vol. 13, pp. 125–132, 1990.

[15] Stacey M.T. and Ralston A.K., "The scaling and structure of the estuarine bottom boundary layer," *Journal of Physical Oceanography*, vol. 35 pp. 55–71, 2005.

[16] Pope, S. B., *Turbulent Flows*. Cambridge University press, 771 pp., 2000.

[17] J.H. Trowbridge, "On a technique for measurement of turbulent shear stress in the presence of surface waves," *Journal of Atmospheric and Oceanic Technology*, vol. 15, pp. 290–298, 1998.

[18] W.J. Shaw and J.H. Trowbridge, "The direct estimation of near-bottom turbulent fluxes in the presence of energetic wave motions," *Journal of Atmospheric and Oceanic Technology*, vol. 18, pp. 1540-1557, 2001.

[19] J.L. Lumley and E.A. Terray, "Kinematics of turbulence convected by a random wave field," *Journal of Physical Oceanography,* vol. 13, pp. 2000-2007, 1983.

[20] J. H. Trowbridge and S., Elgar, "Turbulence Measurements in the Surf Zone," *Journal of Physical Oceanography*, vol. 31, pp. 2403-2417, 2001.

[21] H. Tennekes and J. Lumley, *A First Course in Turbulence*, The MIT press, 300 pp., 1972.

[22] W.M.J. Batten, A.S. Bahaj, A.F. Molland, J.R. Chaplin, "The prediction of the hydrodynamic performance of marine current turbines." Renewable Energy, vol. 33, pp. 1085-1096, 2008.